Refractive Index Profile of Polyethylene Fiber Using Interactive Multiple-Beam Fizeau Fringe Analysis

A. A. HAMZA,[1] T. Z. N. SOKKAR,[1] M. A. MABROUK,[2] M. A. EL-MORSY[2]

[1] Physics Department, Faculty of Science, University of Mansoura, Mansoura, Egypt

[2] Physics Department, Faculty of Science, Demietta, University of Mansoura, Demietta, Egypt

Received 11 May 1999; accepted 18 May 1999

ABSTRACT: A multiple-beam interference Fizeau fringes technique is used to measure the refractive index profile of drawn polyethylene fiber. The interference fringe shift in the fiber region has been analyzed automatically using an interactive algorithm. The method takes into consideration the refraction of the light beam when crossing the fiber. Plane polarized light vibrating parallel and perpendicular to the fiber axis are used to obtain the refractive index profiles of both cases. These profiles are used to determine some optical parameters such as the birefringence, the optical orientation function, the polarizability per unit volume, and the value $\Delta\alpha/3\alpha_o$, which related to the material structure. The reliability of the method is tested considering the results of drawn polyethylene fiber samples using the manual technique. © 2000 John Wiley & Sons, Inc. J Appl Polym Sci 77: 3099–3106, 2000

Key words: refractive index profile; polyethylene fiber; multiple-beam Fizeau fringe analysis

INTRODUCTION

Multiple-beam interference of the Fizeau type is used by numerous authors to investigate textile and optical fibers.[1–4] Fiber investigation using this technique gives accurate results due to the sharpness of the interference fringes compared with two-beam interference. The methods in which a matching immersion liquids are used give good results on fiber refractive index profiles, especially when both liquid and fiber cladding have refractive indices close to each other. However, it is essential to take the effect of refraction of the beam through the liquid/fiber interface into consideration[4–6] to minimize the error in the measured data.

Correspondence to: M. A. Mabrouk.

Journal of Applied Polymer Science, Vol. 77, 3099–3106 (2000)

Automatic fringe pattern analysis is a powerful and inexpensive digital image-processing technique. It is used in many areas such as aerodynamics,[7] metrology and nondestructive testing,[8] and fiber investigation.[9] In fact, the source of producing the fringe pattern has little or no effect on the analysis algorithm.[10] The multiple-beam interference manual technique, used in fiber characterization, is a time-consuming process because the interferogram must be photographed, enlarged to a suitable magnification then the required data are obtained from the magnified image. These data can be obtained accurately and faster by analyzing the interference fringes with the aid of a computer program to determine the refractive index profile of the fiber.

In this article, an interactive fringe pattern analysis system is used with prepared software by ourselves, to measure (in a few minutes) the refractive index profile and some structural parameters as the optical orientation function, po-

larizability per unit volume and the value ($\Delta\alpha/3\alpha_o$), where $\Delta\alpha$ is the principal polarizability difference of one molecule, and α_o its isotropic polarizability. The possibility to capture a frame every 30 s makes the system able to detect any short time changes in the interferogram.

THEORY

Multiple-beam interference fringes of the Fizeau type can be produced by introducing the sample in a wedge interferometer.[2–4] The wedge interferometer consists of two silver-coated optical flats mounted in a special jig and including the fiber between them. The fiber is immersed in a liquid of suitable refractive index n_L. Both the wedge angle ε and the interferometric gap thickness t are adjusted to produce sharp parallel fringes perpendicular to the fiber axis.

Considering the refraction of the incident ray as it crosses the liquid/fiber interface, the fiber refractive index profile can be obtained accurately. In this method, the fiber cross-section is assumed to be divided into very small circular zones. For a large number of layers (zones), each layer can be considered to have a constant refractive index. The interference fringe shift Z_Q of the Q-th layer in the fiber region is related to the refractive index n_Q of this layer as[4]

$$\frac{\lambda Z_Q}{2h} = \sum_{j=1}^{Q-1} 2n_j\{\sqrt{(R-(j-1)a)^2-(d_Q n_o/n_j)^2} - \sqrt{(R-ja)^2-(d_Q n_o/n_j)^2}\} + 2n_Q\sqrt{(R-(Q-1)a)^2-(d_Q n_o/n_Q)^2} - n_o\{\sqrt{R^2-d_Q^2}) + \sqrt{R^2-X_Q^2}\} \quad (1)$$

where λ is the wavelength of light used, h is the interfringe spacing, R is the fiber radius, a is the layer thickness ($a = R/Q$), $n_o = n_L$ is the immersion liquid refractive index, X_Q and d_Q are the emerged and incident rays distances from the fiber center, respectively, where

$$d_Q = \frac{n_Q\left(R-\left(Q-\frac{1}{2}\right)a\right)}{n_o} \quad (2)$$

The value of Z_Q is given as a function of X_Q along the fiber radius and, hence, the left-hand side if eq. (1) is known at any point X_Q. A suggested value of n_Q is used to calculate the corresponding value of d_Q, and both the values are used to obtain the right-hand side of eq. (1). If the right- and left-hand sides are different, a new value of n_Q is suggested, and the iteration continued until the difference between the left-hand and right-hand sides satisfy the sufficient accuracy of n_Q. Measuring n_Q from $X = R$ to $X = 0$, the refractive index profile of the multilayer graded index optical fiber, considering the refraction of the light beam when crossing the fiber, is obtained. Although such a technique might be used to study the properties of graded index optical fibers, it also gives good results for fibers of simpler structures such as those in textiles with refractive index profiles are, radially, relatively flat.

The term image simply refers to a two-dimensional light intensity function, denoted by $f(x, y)$, where its value or amplitude at spatial coordinates (x, y) gives the intensity (brightness) of the image at that point. The function $f(x, y)$ must be nonzero and finite. Suppose that a continuous image $f(x, y)$ is denoted by the form of an $N \times M$ array, where each element of the array is a discrete quantity:

$$f(x, y) = \begin{bmatrix} f(0,0) & f(0,1) & \cdots\cdots & f(0, m-1) \\ f(1,0) & f(1,1) & \cdots\cdots & f(1, m-1) \\ \vdots & & & \\ \vdots & & & \\ f(n-1, 0) & & & \\ f(n-1, 1) & \cdots\cdots & & f(n-1, m-1) \end{bmatrix}$$

Each element of the array is referred to as an image element, picture element or pixel.[11] To be suitable for computer processing, the image function $f(x, y)$ must be digitized both spatially and in amplitude. Digitization of the spatial coordinates (x, y) is called image sampling, and amplitude digitization is called gray-level quantization. The flow chart of the method followed in this work is shown in Figure 1.

Image Segmentation

When the image is divided into different regions (two or more), this process is called "Image Segmentation." It is not concerned with the region characteristics, but it means the process of partitioning the image. The simplest case of image

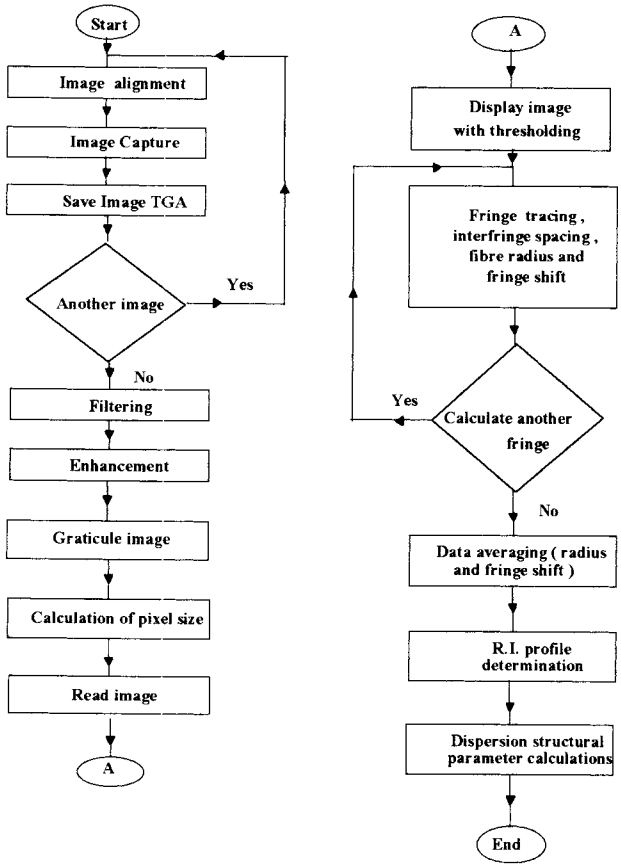

Figure 1 The flow chart of the method applied.

segmentation is to have only two regions called thresholding, which is one of the most important approaches to image segmentation.[11,12]

Single-band thresholding (fixed thresholding) assumes that the objects have pixel values generally different from the background. A binary output image containing only 0s (background) and 1s (object), may be created by applying a thresholding[13]:

$$V_{\text{out}} = \left\{ \begin{array}{ll} 0 & \text{if } V_{\text{in}}(i,j) < \text{threshold} \\ 1 & \text{otherwise} \end{array} \right\}$$

where, V_{in} is the pixel value at the gray-level and V_{out} is the pixel value at the binary level.

The System Magnification and Pixel Size

A graticule is used to determine the system magnification and the image pixel size. The pixel size plays an important rule in image resolution and calculating its value means, converting the image element dimensions to real values in microns. The image intensity and magnification of the system are adjusted to provide as small a pixel size as possible. The smaller is the pixel size, the higher is the measurement accuracy.

Fringe Tracing

Fringe tracing is the most important procedure in the fringe analysis process. The image is displayed in such a way that the fiber is parallel to the vertical direction and the fringes are in the horizontal direction. A scanning of the image vertically enables one to detect the width and coordinates of the chosen fringe, which is filled with a specific color. This process determines the edges of the chosen fringe (edge detection of the fringe). Along the detected edges of the fringe, the average of vertical points gives an intermediate contour line in both the liquid and fiber regions. To increase the accuracy of the measured data, the contour lines of four successive fringes (or more) are used to get the average contour line to avoid the error due to fringe irregularity.

Calculation of the Refractive Index Profile and Optical Parameters

The automatically measured data (fiber radius, interfringe spacing, and the fringe shift curve as a function of radius) are averaged and used in eq. (1) to get the refractive index profile of the fiber interactively. The measured interference fringe shift points (Z_Q) as a function of the fiber radius are fitted using a polynomial equation to give a continuous curve, relates Z_Q with its corresponding point X along the radius. The resulting curve is important for the iteration used in eq. (1), to obtain the fiber refractive index profile.[4] A comparison between the automatically measured refractive index profiles and those measured manually using enlarged patterns are presented.

Plane polarized monochromatic light vibrating parallel ($\|$) and perpendicular ($\perp$) to the polymer fiber axis are used to get the refractive index profile $n_{\|}(r)$ and $n^{\perp}(r)$, respectively. These profiles are used to obtain the fiber optical parameters such as the optical orientation function profile, birefringence, polarizability per unit volume profile, and the value $(\Delta\alpha)/(3\alpha_o)$, which is related to the fiber material structure.

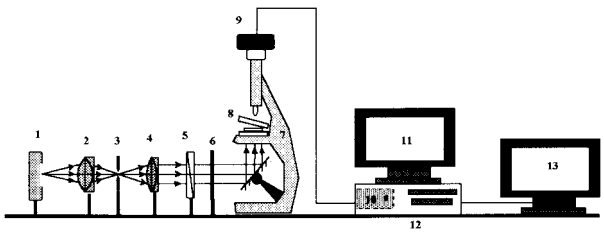

Figure 2 The optical setup that produces multiple-beam Fizeau fringes attached with the image acquisition system.

OPTICAL SETUP AND IMAGE ACQUISITION SYSTEM

The set up of multiple-beam Fizeau fringes in transmission, which produces microinterferograms characterized by sharp, bright fringes in a dark background, is shown in Figure 2. The interferometer is adjusted in such a way that the fiber is exactly perpendicular to the interference fringes in the liquid region. The accuracy of the refractive index profile, and hence, the structural parameters measurement, are affected by the deviation of the fiber and fringes from the right angle. Deviation from the right angle by one degree or less causes a negligible change in the measured quantity.[9]

A PC with a 486 microprocessor and a Panasonic CCD video camera with an attached frame grabber digitizer of 512 $\times$ 512 bytes are used to digitize the interferogram directly from the microscope. A crosshair is used to adjust the fiber to be perpendicular to the fringes. A relay lens is inserted between the microscope and the CCD camera to sharpen the interferogram.

The digitized image is then captured and saved as a TGA image file format. This simplest form of image format is called the targa (TGA) format, according to which the file consists of three regions: the first is a fixed length of an 18 bytes header that contains information about the image such as size, color, number of both rows, and columns. The image data represents the second part of the file, while the third part is the color palette, which represents the list of the image colors.[14] It is preferred to deal with images of a gray-level format in the area of fringe analysis, so the saved TGA color format can be converted to a gray-level one.

RESULTS AND DISCUSSION

Image Enhancement and Contour Line Tracing

During the image enhancement process, data distortion or reduction are produced whatever the accuracy of the image processing technique applied.[15] The captured images of multiple-beam interference Fizeau fringes using the CCD camera are shown in the right patterns of Figures 3(a), 3(b), and 3(c). These interferograms are produced using polyethylene fiber samples, which are drawn to different draw ratios. The draw ratio Λ is the ratio of (ℓ'/ℓ), where ℓ is the fiber original length and ℓ' is the fiber length after drawing, i.e., $\Lambda = \varepsilon + 1$ and ε is the strain. The samples used in Figures 3(a), 3(b), and 3(c) are drawn to 7.5, 10, and 12.5, respectively. Monochromatic light (λ = 546.1 nm) vibrating parallel to the fiber axis is used, and the immersion liquids used are of refractive n_L = 1.5787, 1.5849, and 1.5870, respectively. Image thresholding gives good pattern segmentation, as shown in the middle patterns of Figures 3(a), 3(b), and 3(c).

It is known that when applying a thresholding process, it removes (or adds) some of the image noises.[13] One can notice that applying the thresholding process on the right patterns, some of the image noises were added to (or reduced from) data on the fringe borders, which cause some irregularity on it, as shown in the middle patterns. The middle patterns are filtered to reduce this irregularity, and the images of the left patterns are produced. The enhanced interferograms shown in the left side of Figure 3(a), 3(b), and 3(c) are used to obtain the fringe contour lines by automatic fringe tracing, as shown in Figure 4. The contour lines are traced along the chosen fringes, while the average of (at least) four fringes was fitted and plotted beside the chosen fringes as shown in Figure 4(a), 4(b), and 4(c).

Refractive Index Profile and Fiber Optical Parameters Measurement

Refractive index profiles of drawn polyethylene fibers were obtained using both automatic fringe analysis and the manual technique measurement. In the automatic technique, the reliability of the presented algorithm is tested for three dif-

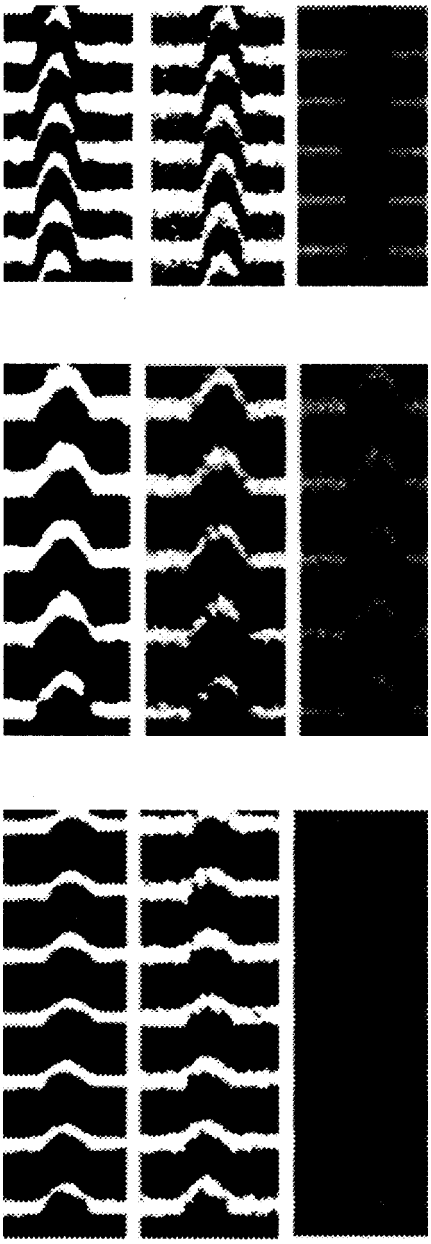

Figure 3 Microinterferograms of polyethylene fibers with draw ratios (a) 7.5, (b) 10, and (c) 12.5. Light of $\lambda = 546.1$ nm vibrating parallel to the fiber axis is used (at right side). The interferograms after thresholding are shown in the middle, and applying a suitable filter gives the patterns on the left.

ferent filaments of the sample having a draw ratio 10 and light vibrating parallel to the fiber axis. The measured refractive index profiles in this case show good agreement with each other (see Fig. 5) considering the experimental errors in immersion liquid measurement, small temperature changes, core radius tolerance, and errors due to image enhancement.

The fiber samples and conditions used in Figure 3(a), 3(b), and 3(c) are used to determine the refractive index profiles of drown polyethylene fibers, using automatic and manual techniques, as shown in Figure 6(a), 6(b), and 6(c). The automatic technique shows better accuracy than the

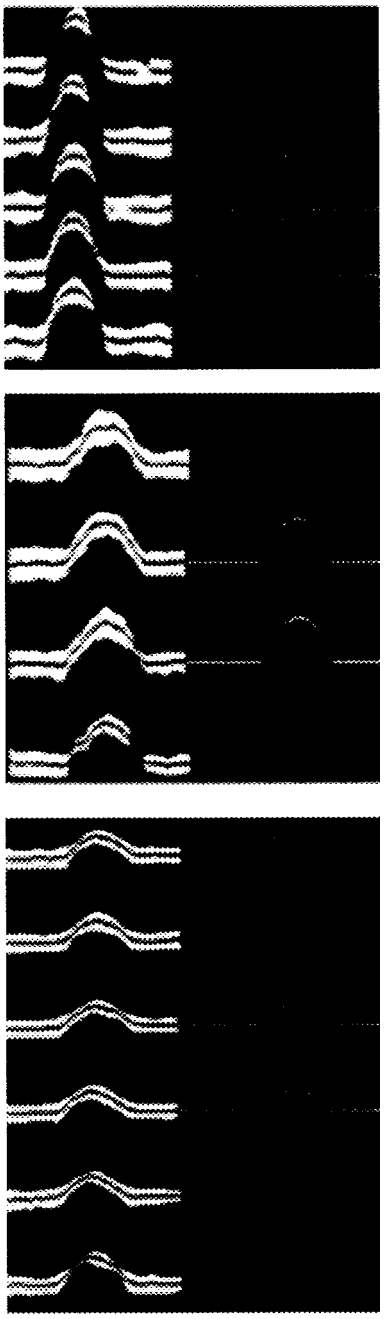

Figure 4 The contour lines traced along a chosen fringes, while its average were fitted and plotted beside the fringes, the microinterferograms used are shown in Figure 3.

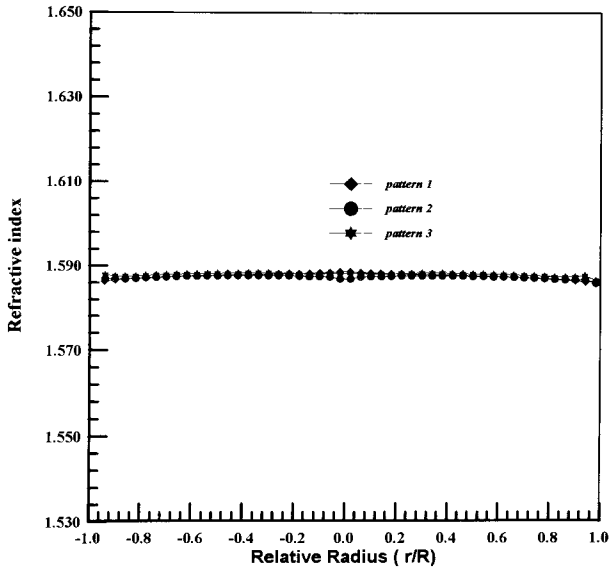

Figure 5 Refractive index profile measurement of a sample having a draw ratio of 10 using three different interferograms at nearly the same condition.

manual technique. In fact, the refractive index profile of the polyethylene fiber is nearly flat, and it is clear that the automatic measurements tend to be more flat than the manual ones, as shown in Figures 6(a), 6(b), and 6(c).

The use of immersion liquid n_L, with refractive index far from that of the fiber, influences also the accuracy of the measured data. For instance, the interference fringe shift in the fiber region is about one interference order as shown in Figure 3(a), which gives a big difference between manual and automatic measurements. This difference decreases as the used immersion liquid refractive index become close to the fiber refractive index [see Fig. 3(c)], which is the case of refractive index profiles shown in Figure 6(c). For the manual technique, when the fringe shift has a comparatively large value, the probability of the errors in the measured profile increases, and when it has small value a minimum error is obtained. These results conclude that automatic measurement technique is recommended when the immersion liquid used has refractive index far from that of the fiber or when the interference fringe shift value is large.

The difference between the results of both methods can also be explained in terms of the measurement unit length used. In this work, the interferogram, in the case using the manual technique, is enlarged so that the unit length of 1 mm used along the interferogram has a 3.15-μm real size. On the other hand, the unit length used in the automatic technique is the pixel, which is 1.3 μm in most measurements, which increases the accuracy. Similar results on refractive index profile $n(r)$ are obtained for the same fiber samples when using monochromatic light vibrating perpendicular to the fiber axis.

The refractive index profiles $n^{\parallel}(\boldsymbol{r})$ and $n^{\perp}(\boldsymbol{r})$ of the fiber at certain draw ratio are calculated as a function of $(\boldsymbol{r/R})$. So, at a certain point $(1 \geq (\boldsymbol{r/R}) \geq 0)$ along the fiber radius both $n^{\parallel}(\boldsymbol{R/R})$ and $n^{\perp}(\boldsymbol{r/R})$ are known and, hence, the birefringence can be calculated.

The maximum birefringence is the birefringence of the fully oriented polymeric fiber. For polyethylene fiber, the value of maximum birefringence $\Delta n_{\max} = 0.0735$ was reported by Pietralla and Grossman.[16] This value is used to get the refractive indices of fully oriented fiber, n_1 and n_2,[17] and they are found to be $n_1 = 1.6021$ and $n_2 = 1.5286$. These values were used to automatically obtain the optical orientation function profiles for polyethylene fiber at three different values of draw ratios as shown in Figure 7.

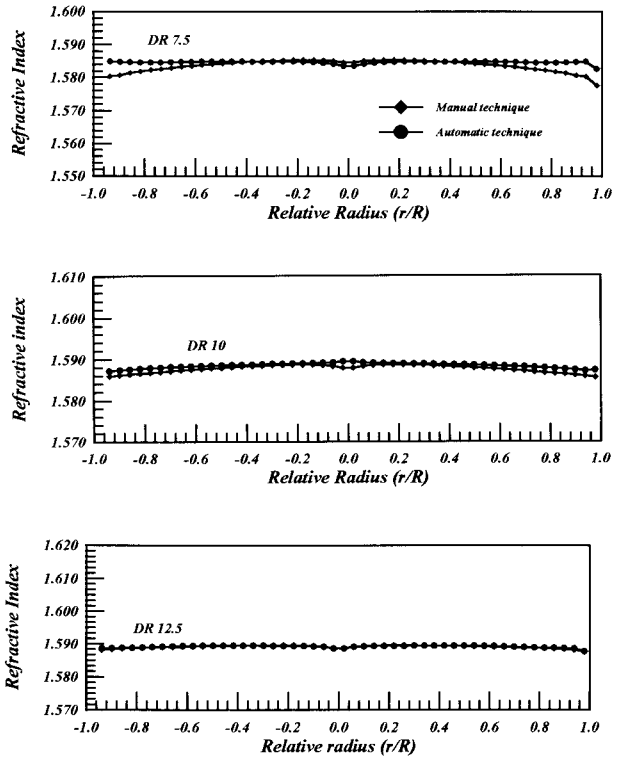

Figure 6 The refractive index profiles of drawn polyethylene fibers with draw ratios of (a) 7.5, (b) 10, and (c) 12.5, using a monochromatic light vibrating parallel to the fiber axis.

One can notice that the orientation function $f(\theta)$ increases as the draw ratio increases.

The polarizability per unit volume along the polyethylene fiber radius when using light vibrating parallel to the fiber axis, is found to be increased with the draw ratio, and when using light vibrating perpendicular to the fiber axis, it is found to be decreased as shown in Figure 8.

The value $(\Delta\alpha)/(3\alpha_o)$ measured automatically for drawn polyethylene fibers is found to have constant value (independent on the draw ratio) and found to be 0.0366, which is nearly equal to the value measured using other methods.[18]

CONCLUSION

Multiple-beam interference Fizeau fringes automatic analysis is used to obtain the refractive index profile of textile fibers. Fast analysis is used to investigate the fiber interferometrically. A monochromatic light beam vibrating parallel and perpendicular to the fiber axis helps to obtain the refractive index profile for each case. These profiles are used in the same algorithm to obtain some optical parameters, as the optical orientation function, the polarizability per unit volume profile, and the value $(\Delta\alpha)/3\alpha_o)$, which is related to the fiber molecular structure.

The reliability of the method is tested using three different filaments of the same sample to make three different interferograms, and compared to the results with respect to each other. Although there were some little differences in the experiment temperature and there is a tolerance in the fiber radius measurements, the measured refractive index profiles are nearly equal.

The algorithm of the method used enables one to determine more than one fringe shift and averaging them over their numbers, and hence, the accuracy of the measurement is increased. Using an immersion liquid of the refractive index near to the fiber one, the produced fringe shift in the fiber region would be small, and both the liquid and fiber fringes are continuous. For this case, a continuous contour line is produced that also increases the accuracy of the measurements.

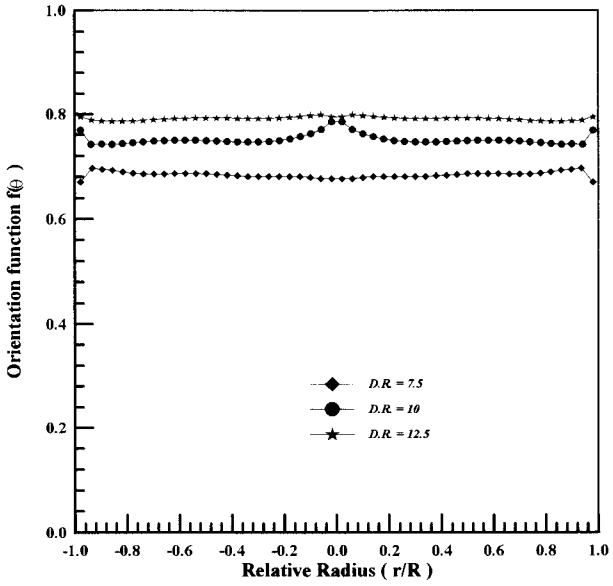

Figure 7 The optical orientation function $f(\theta)$ as a function of the relative radius (r/R).

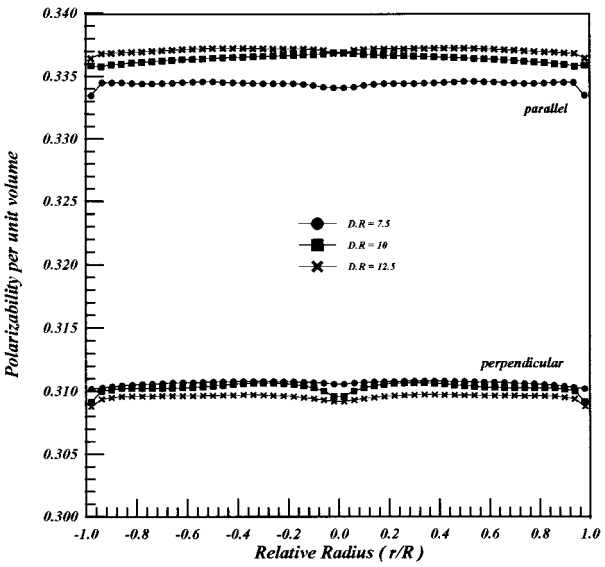

Figure 8 The polarizability per unit volume measured along the fiber radius for drawn polyethylene fibers with draw ratios of 7.5, 10, and 12.5, and when the light beam is vibrating parallel and perpendicular to the fiber axis.

REFERENCES

1. Faust, R. C. Physical Methods of Investigation Textiles; Textile Book Pub. Inc.: New York, 1959.
2. Barakat, N.; Hamza, A. A. Interferometry of Fibrous Materials; Adam-Hilger: Bristol, 1990.
3. Barakat, N.; Hamza, A. A.; Gonied, A. S. Appl Opt 1985, 24, 4383.
4. Hamza, A. A.; Sokkar, T. Z. N.; Ghander, A. M.; Mabrouk, M. A.; Ramadan, W. A. Pure Appl Opt 1995, 4, 161.
5. Kowalik, W.; Dubik, B. Opt Appl 1990, 20, 3.

6. Sochacki, J. Appl Opt 1986, 25, 3473.
7. Becker, F.; Yu, Y. H. Opt Eng 1985, 24, 429.
8. Kujawinska, M.; Robinson, D. W. Appl Opt 1988, 27, 312.
9. Roche, E. J.; Rubin, B.; Van Kavelaar, R. F. Text Res J 1987, 57, 371.
10. Reid, G. T. SPIE 1988, 954, 468.
11. Gonzalez, R. C.; Wood, R. E. Digital Image Processing; Addison-Wesley Pub.: New York, 1993.
12. Sid-Ahmed, M. A. Image Processing: Theory, Algorithms and Architectures; McGraw Hill Inc.: New York, 1995, p. 5.
13. Niblack, W. An Introduction to Digital Image Processing; Prentice/Hall International: London, 1985, p. 10.
14. Heing, L. Advanced Graphics Programming Using C/C++; John Wiley and Sons Inc.: New York, 1993.
15. Allred, L. G.; Kelly, G. E. SPIE 1992, 1702, 285.
16. Pietralla, M.; Grossmann, H. P. J Polym Sci Polym Phys Ed 1982, 20, 1193.
17. de Vries, H. Colliod Polym Sci 1979, 257, 226.
18. Mabrouk, M. A.; Shams-Eldin, M. A. Pure Appl Opt 1996, 5, 929.